How to Cite: Shakhabutdinov, S.Sh., Yugay, S.M., Ashurov, N.Sh., Ergashev, D.J., Atakhanov, A.A., & Rashidova, S.Sh. (2024) Characterization Electrospun Nanofibers Based on Cellulose Triacetate Synthesized from Licorice Root Cellulose. *Eurasian Journal of Chemistry*, *29*, *2(114)*, *21-31*. https://doi.org/10.31489/2959-0663/2-24-2

Article

Received: 15 January 2024 | Revised: 22 April 2024 |
Accepted: 24 April 2024 | Published online: 7 May 2024

UDC 677.464.1

https://doi.org/10.31489/2959-0663/2-24-2

Siroj Sh. Shakhabutdinov, Svetlana M. Yugay, Nurbek Sh. Ashurov, Doniyor J. Ergashev, Abdumutolib A. Atakhanov*, Sayyora Sh. Rashidova

Institute of Polymer Chemistry and Physics, Tashkent, Uzbekistan
*(*Corresponding author's e-mail: a-atakhanov@yandex.com)*

Characterization Electrospun Nanofibers Based on Cellulose Triacetate Synthesized from Licorice Root Cellulose

Cellulose triacetate (CTA) nanofibers were formed by electrospinning using two binary solvent systems: methylene chloride/ethanol and chloroform/acetone. Previously, licorice root cellulose (LRC) with a degree of polymerization (DP) of 710 was extracted from licorice root waste by alkaline treatment and hydrogen peroxide bleaching at high temperatures. Then CTA with a degree of substitution (DS) of 2.9 and an average molecular weight of 175 kDa was synthesized from LRC using acetic acid and acetic anhydride, sulfuric acid was as a catalyst. The influence of the electrospinning process and various solvent systems on the morphology and structure of nanofibers was studied. The structure and morphology of the nanofibers were characterized by Fourier transform infrared (FTIR) spectroscopy, X-ray diffraction, scanning electron microscopy (SEM), thermal gravimetric analysis (TGA), and the sorption characteristics were also investigated. The results showed that the morphology and structure of nanofibers depended on the solvent mixture used. The average diameters of the CTA nanofibers with grooved morphology varied 200–700 nm (solvent methylene chloride/ethanol) and the dumbbell-shaped (flat ribbon) CTA nanofibers in a wide range from 200 nm to 4 mkm (solvent chloroform/acetone).

Keywords: electrospinning, cellulose triacetate, nanofibers, X-ray diffraction, FTIR, degree of crystallinity, sorption, thermal stability.

Introduction

As an eco-friendly and renewable biopolymer on the earth, cellulose gains an extensive interest in producing novel polymer materials. In this foreshortening, cellulose- and its derivatives-based fibres and nanofibres are very attractive because of their high strength and firmness, biodegradability and safety [1–5].

Cellulose can be extracted from different native sources, such as wood, cotton, flax, hemp, ramie, etc. [6–8]. In recent years, there has been an increasing trend towards extracting cellulose from agro-industrial wastes. The properties and structure of cellulose derived from these wastes vary considerably and can be used in different industrial sectors [9-10]. One of such agro-industrial waste is licorice root which consists of about 40–45 % cellulose. Products based on licorice root are used to treat ailments like heartburn, acid reflux, hot flashes, coughs, and bacterial and viral infections [11]. After separating the medicinally active component from the licorice root using selective solvents, a large mass of fibre waste remains, which can be used as raw material for the cellulose and paper [12]. Using cellulose extracted from licorice root waste offers several advantages compared to traditional sources like wood or cotton. Licorice root waste provides an alternative source of cellulose that utilizes a byproduct of the licorice industry, reducing waste and promoting sustainability. Unlike wood, which requires deforestation, or cotton, which requires extensive water and pesticide usage, licorice root waste repurposes a material that would otherwise be discarded.

The cellulose derivatives having different functional groups in the cellulose chain have great demand, and some of them, including cellulose acetate, are produced in large quantities. Cellulose acetate can be used for producing membranes, packaging films, optical devices, and polymer composites [13, 14]. Usually, conventional spinning methods such as melt spinning, wet spinning, dry spinning, and gel spinning are used for forming cellulose acetate fibres with a few microns in diameter. However, a breakthrough came with the advent of electrospinning, which allowed researchers to produce ultrathin fibre [15]. Electrospinning is an electrohydrodynamic method used for producing synthetic and natural polymer fibres by electrical force, gathering significant interest due its ability to produce fibres at the nanoscale [16]. Electrospinning of nanofibers is

an attracting method to fabricate cellulose acetate membranes with large surface, high porosity and they have been extensively used in biomedicine, filtration and protection, energy storage and energy catalyst [17].

In this work, cellulose was extracted from licorice root waste, and then cellulose triacetate (CTA) was synthesized based on it. The CTA nanofibres were formed by the electrospunning method using new solvent systems as a mixed solvent of methylene chloride:ethanol and chloroform:acetone, and their structure and morphology were investigated.

Experimental

Chemicals and Materials

The following chemicals and materials were used: sodium hydroxide (NaOH, 99 %), hydrogen peroxide (H_2O_2, 60 %), sodium hypochlorite (17 %), sulfuric acid (H_2SO_4, 95–97 %), nitric acid (HNO_3, 65 %), hydrochloric acid (HCl, 37 %) were purchased from "Himreactiv invest" Company Ltd., Uzbekistan Acetic acid (CH_3COOH, 99 %), ethanol (C_2H_5OH), acetone ($(CH_3)_2CO$) were purchased from "Fortek" Company Ltd., Uzbekistan Acetic anhydride ($(CH_3CO)_2O$, 99.5 %), methylene chloride (CH_2Cl_2), chloroform ($CHC1_3$) were purchased from Sigma–Aldrich, USA.

Cellulose Extraction

The cellulose was isolated from wastes. It is a complex procedure that involves chemical or mechanical methods and sometimes a combination of both of them. The licorice root waste was treated in 4 % sodium hydroxide solution at 120 °C for 2 h to remove noncellulose substances (hemicellulose, lignin etc.), as reported previously [3]. Then the mass was washed with deionized water three times (the pH of the solution was neutral) and bleached in 4 % hydrogen peroxide solution at 120 °C for 2 h. The bleached product was separated by filtering, and washed three times with deionized water and dried in the drying oven at 100 °C for 4 h. The degree of polymerization (DP) of LRC was 710, and it was used for the synthesis of the CTA.

Cellulose Triacetate Preparation

The acetylation of LRC was carried out using an acetic acid and acetic anhydride in the presence of sulphuric acid as catalyst [18]. Briefly, 2.5 g of licorice root cellulose (LRC) was placed in a flask with a ground stopper and treated with a mixture pre-cooled to 15 °C with 15–20 ml of acetic acid, 0.5 ml of H_2SO_4, and 10–20 ml of acetic anhydride. The mixture was left to stand for 2 days at room temperature (or 4 hours at 40 °C). During this time, the formation of syrup (a viscous concentrated solution of cellulose acetate) occurs. The resulting thick syrup was diluted by half with glacial acetic acid and poured into a large vessel with ice water. This produces white flakes of cellulose triacetate, which were left in water for 24 hours to decompose completely the acetic anhydride. After this time, cellulose triacetate was filtered, washed, and dried at 95–100 °C. CTA had DS of 2.9, average molecular weight of 175 kDa.

Solution Preparation

CTA solutions were prepared from CTA samples that previously were condensed in a vacuum oven at 80 °C for about 8 h. CTA solutions were prepared by dissolving CTA in solvent mixtures at 25 °C with constant stirring for 2 h. As a solvent the mixtures methylene chloride:ethanol (9:1) (CTA-NF-1) and chloroform:acetone (9:1) (CTA-NF-2) were used.

Electrospinning of CTA Nanofibers

The fabrication of nanofibers was carried out by the electrospinning machine NanoNCeS-robots (South Korea). Elestrospinning conditions were the following: the applied voltage was 25 kV, the needle tip and collector distance was 14 cm; the needle diameter was 0.353 mm; the rate of the injecting solution was 45 mkl/min. During the spinning process the relative humidity was 60 % and temperature was 25 °C. The electrospun CTA fibers were vacuum-dried at 60 °C for 1 h.

Characterization Methods

FTIR

The FTIR spectrometer "Inventio-S" (Bruker) was used and FTIR spectra were recorded in 400–4000 cm^{-1} wavenumber range with a resolution of 2 cm^{-1} and 32 scans at a temperature of 25 °C. Software of OPUS was applied to determine the peaks at specific points.

Wide-Angle X-ray Diffraction

XRD studies were carried out using XRD Miniflex 600 (Rigaku, Japan) with monochromatic CuKα radiation isolated by a nickel filter with a wavelength of 1.5418 Å at 40 kV and the current strength of 15 mA. The spectrum was recorded in the interval of $2\theta = 5°–40°$. The data processing of experimental diffraction patterns, peak deconvolution, describing the peaks used by Miller indices, peak shape, and the basis for the

amorphous contribution were conducted using the software "SmartLab Studio II" and data base PDF-2 (2020 Powder diffraction file, ICDD).

Thermogravimetric analysis (TGA)

TG-DSC/DTA synchronous thermal analyzer STA PT1600 (Linseis, Germany) was used for thermal analysis of the samples. The process was carried out by heating ~ 20 mg of the sample in an air atmosphere at a heating rate of 10 °C/min from 25 °C to 900 °C. The samples were previously dried to constant weight.

SEM

Scanning electron microscopy studies were performed using SEM equipment Veritas-3100 (Korea). Magnification of the device is x10-300000, voltage 200V–300V, maximum scanning area (x÷y÷z) is 120÷120÷65 μm.

Sorption Measurements

The McBain balance with quartz spirals of 1 mg/mm sensitivity was used for the sorption investigation. Measurements were carried out in the relative humidity (P/Ps) range 0.10–1.0 at 25 °C until sorption equilibrium was established. KM-8 cathetometer was used for observing the change in sample mass during the sorption process.

Statistical analysis

All experimental data were collected in triplicates and data expressed as average ± standard deviation. Data were compared using a one-way ANOVA with post-Bonferroni test using GraphPad Prism 5.04 (GraphPad Software Inc.)

Results and Discussion

Electrospinning has important tunable working parameters (solution, process and ambient parameters) that can affect the fiber diameter and morphology. With control and proper manipulation of these parameters, one can produce electrospunnanofibers with desirable physical properties for advanced applications [19].

The FTIR spectra of LRC (Fig. 1) have all peaks corresponding to cellulose structure [3]. Around 3400 cm^{-1}, valence vibrations of the hydroxyl groups engaged in intra- and intermolecular hydrogen bonding were visible. The C–H bond valence vibrations in the cellulose methylene groups were observed in the range of 2895 cm^{-1} and 1635 cm^{-1} vibrations of adsorbed water molecules. In the areas of 1420 cm^{-1}, 1335–1375 cm^{-1}, 1202 cm^{-1}, and 1075–1060 cm^{-1}, the absorption bands matched the valence vibrations of the C–O pyranose ring and the strain vibrations of –H, $–CH_2$, –OH, and –CO.

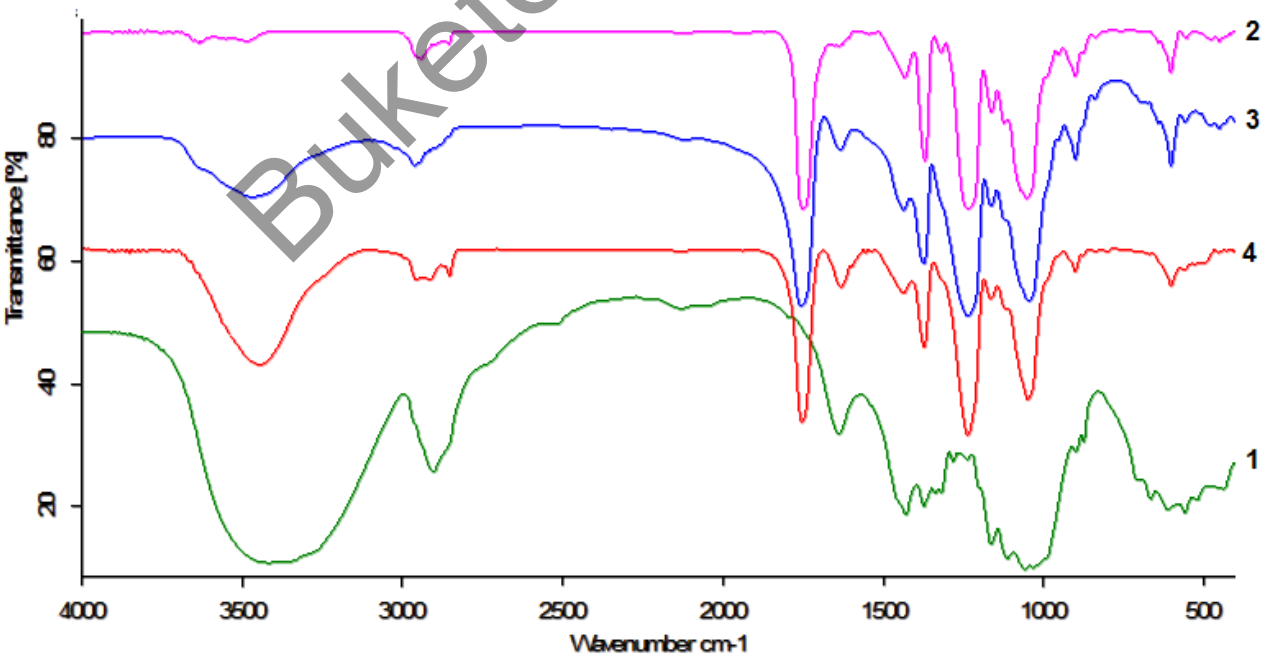

Figure 1. FTIR spectra of LRC (1), CTA (2), CTA-NF-1 (3) and CTA-NF-2 (4)

The FTIR spectrum of CTA typically shows characteristic peaks associated with the acetylated cellulose structure. There is a decrease in the intensity of the –OH absorption band that the hydroxyl group contents in LRC were reduced after esterification. The weakening of peaks related to hydroxyl groups (–OH) in the region (around 3300–3500 cm^{-1}) indicates successful acetylation of cellulose. The ester carbonyl absorption peaks at 1746.6 cm^{-1}, carbonyl hydrogen (C–H) peak at 1374.3 cm^{-1} in acetyl group and 1230 cm^{-1} absorption (C–O) in O–C=O group confirmed that the ester bond have been formed in the CTA and their relative intensity is enhanced. This is in agreement with the author's work in [20] where the characteristic peaks developed confirmed the acetylation of cellulose extracted from cotton stalk.

The FTIR spectra of CTA-NF-1 and CTA-NF-2 show all the peaks characteristic of the CTA, which confirms that the structure of nanofibers is similar as CTA. However, an increase in peak intensity at 3400 cm^{-1} and 1630 cm^{-1} is observed in the spectra of nanofibers, which can be related to the water molecules adsorbed on the active surface of the nanofibers.

The XRD analysis showed of LRC typically exhibits crystalline diffraction peaks corresponding to the native cellulose structure. The presence of well-defined peaks in the XRD pattern indicates the crystalline nature of cellulose in the licorice root material. There are four crystal reflections in the regions of $2\theta = 14^{o}$, 16^{o}, 22^{o} and 34^{o}, corresponding to the planes $1\bar{1}0$, 110, 200, and 004 in the X-ray diffraction patterns (Fig. 2*a*).

The acetylation process of cellulose disturbs the cellulose crystal structure and leads to the decrease in the degree of crystallinity of CTA (Fig. 2(1*b*)) [21]. CTA has a characteristic wide crystal reflection at $2\theta = 15^{o}–30^{o}$, associated with interplanar distances. There are crystalline reflections in the regions of $2\theta = 9.56^{o}$, 17.01^{o}, 18.69^{o}, 29.30^{o} and 39.06^{o}, corresponding to the planes (020), (100), (001), (150) and (022). The functionalization process leads to the change in the supramolecular structure, which becomes orthorhombic with lattice parameters $a = 5.64$ Å, $b = 20.36$ Å, $c = 4.58$Å, $\alpha = \beta = \gamma = 90.00^{o}$.

X-ray diffraction analysis of CTA nanofibers showed (Fig. 2 (2*b* and 3*b*)) that there are regions of coherent scattering at the angles of $2\theta = 10÷15^{o}$ and $20÷25^{o}$. During the electrospinning process, CTA macromolecules organize well-ordered structures, so CTA-NF-1 and CTA-NF-2 nanofibers have a higher crystal index (in the range of 41–46 %) than CTA (Table 1).

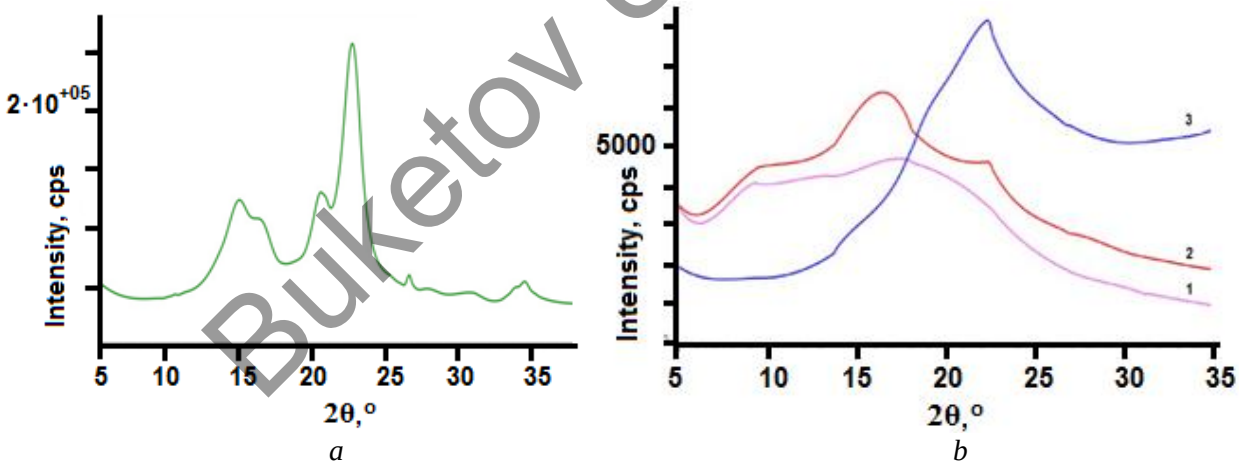

Figure 2. X-ray diffraction patterns of LRC (*a*), CTA (*b*, line 1), CTA-NF-1 (*b*, line 3) and CTA-NF-2 (*b*, line 2)

Table 1

Structural parameters of LRC, CTA, CTA-NF-1 and CTA-NF-2

Sample	Miller indices *hkl*	2θ, deg.	d-spacing, Å	FWHM, °	Crystallite size *τ*, Å	CrI, %	Unit cell size, Å		
							a	*b*	*c*
1	2	3	4	5	6	7	8	9	10
LRC	1-10	14.92	5.93	1.92	43	63	7.81	8.17	10.35
	110	16.40	5.39	1.62	52				
	102	20.69	4.28	1.40	60				

Continuation of Table 1

1	2	3	4	5	6	7	8	9	10
LRC	200	22.76	3.90	1.44	58	63	7.81	8.17	10.35
	103	29.00	3.00	8.00	11				
	113	30.96	2.88	1.83	47				
	004	34.62	2.58	0.99	87				
CTA	020	9.56	9.25	5.20	16	36	5.64	20.36	4.58
	100	17.01	5.21	3.00	30				
	001	18.69	4.75	10.60	8				
	150	29.30	3.05	17.90	5				
	022	39.06	2.0	28.00	3				
CTA-NF-1	100	15.02	5.90	3.90	22	46	6.07	16.04	5.34
	021	20.12	4.41	4.40	19				
	130	22.16	4.01	2.16	39				
	140	26.63	3.35	7.90	11				
	022	35.92	2.49	11.10	8				
CTA-NF-2	020	10.01	8.83	4.75	17	41	3.19	18.09	5.50
	001	16.48	5.38	6.89	12				
	011	17.08	5.18	0.26	325				
	031	22.24	3.99	3.70	23				
	100	28.43	3.13	0.32	271				

The thermal properties of the LCR, CTA, CTA-NF-1 and CTA-NF-2 were studied with TGA (Fig. 3). The weight loss for all investigated samples proceeds in three stages. In the initial stage, occurring at lower temperatures (up to 120 °C), the weight loss (5–9 %) is primarily attributed to the release of adsorbed water (moisture) [5, 22].

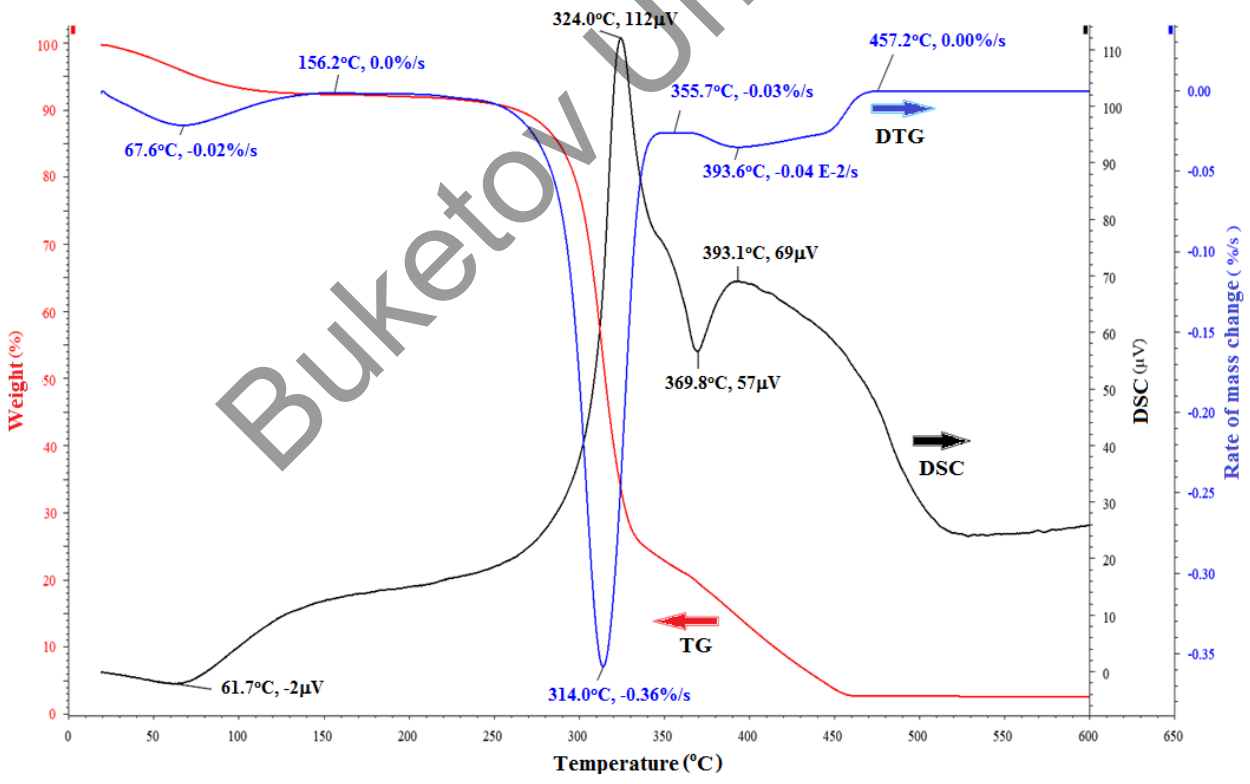

a

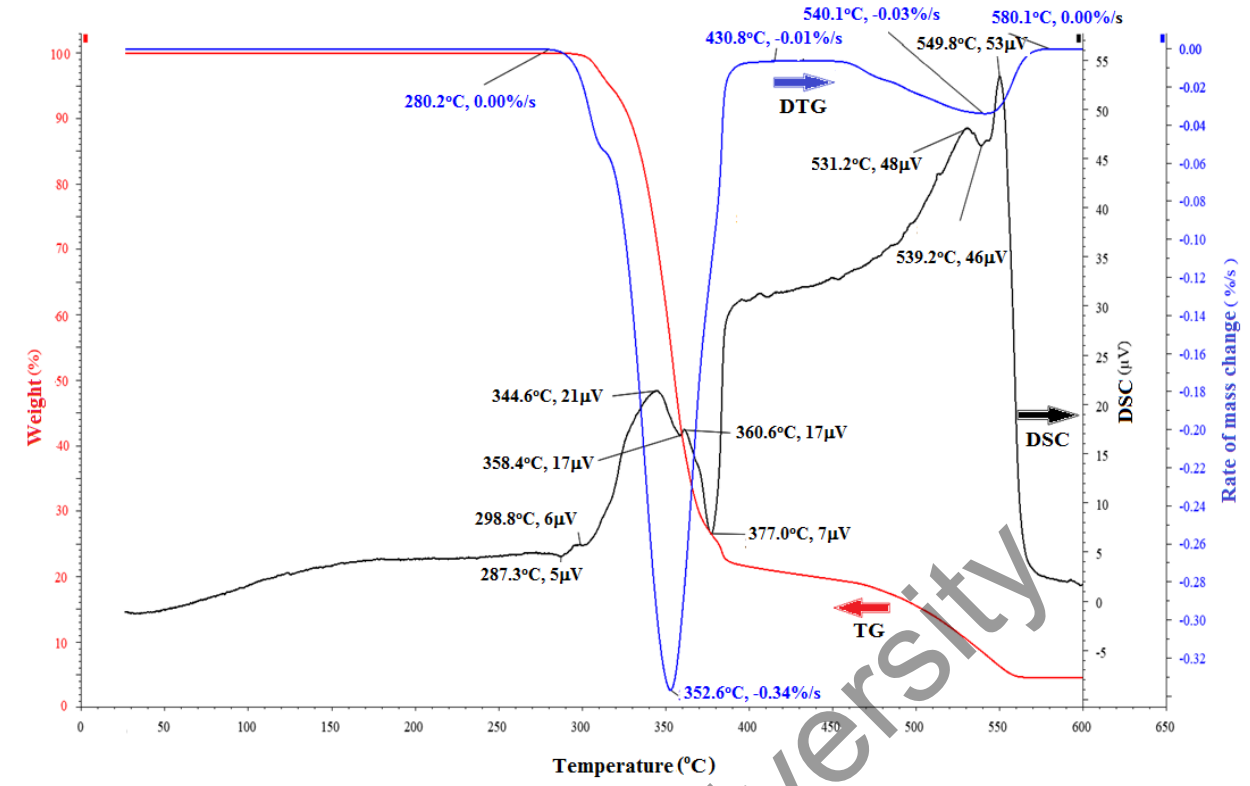

b

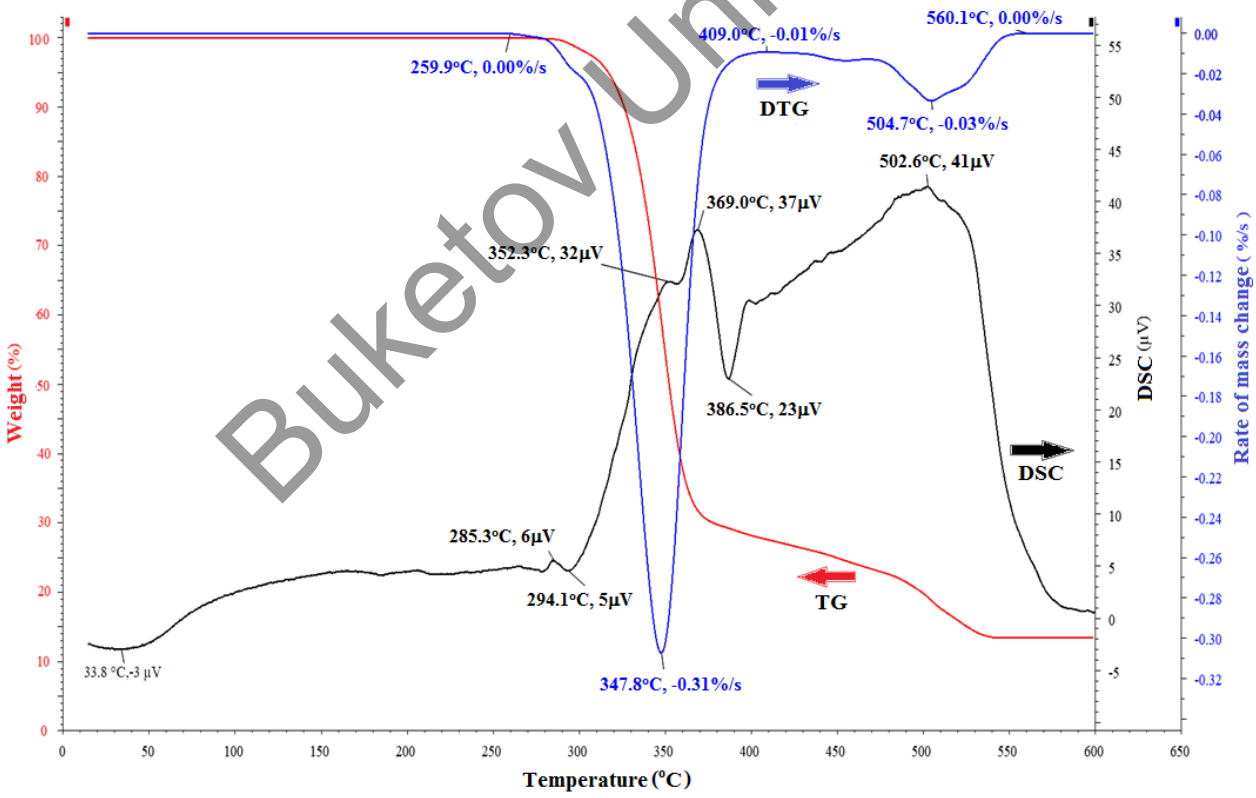

c

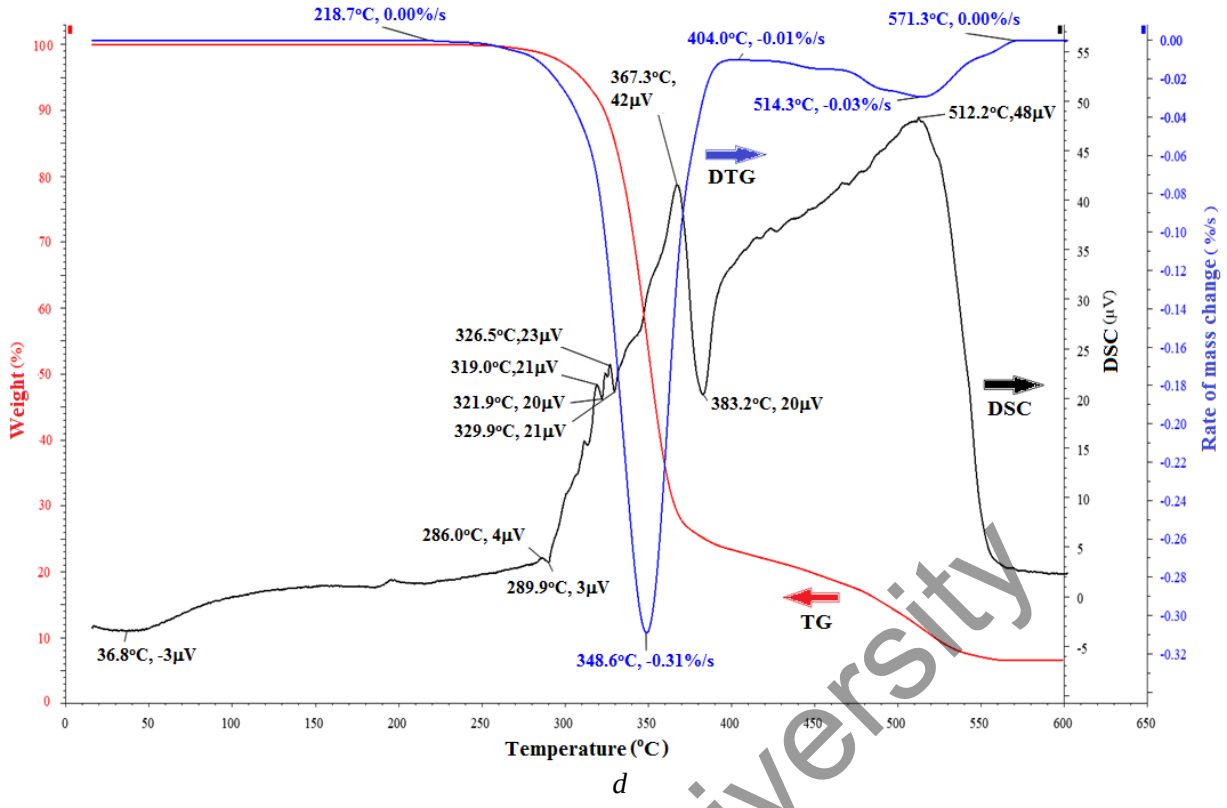

d

Figure 3. TG, DTG and DSC thermograms of LRC (*a*), CTA (*b*), CTA-NF-1 (*c*) and CTA-NF-2 (*d*)

The weight loss was not observed in the CTA, CTA-NF-1, and CTA-NF-2 over the temperature range from 40 °C to 120 °C, indicating that the CTA fibers are more hydrophobic than the LRC. On the weight-loss stage, which took place between 218 and 580 °C, the esterified chains of cellulose acetate are degraded first (in the range of 280–312 °C for CTA, 260–305 °C for CTA-NF-1, 219-280 °C for CTA-NF-2), and then the cellulose chain undergoes the depolymerization process, resulting in the formation of carbon residue [18, 23]. The onset and end thermal degradation temperature of LRC (157–476 °C) are lower than those of the CTA (280–580 °C), CTA-NF-1 (260–560 °C) and CTA-NF-2 (218–571 °C). Moreover, the maximum weight loss rate peak of LCR is also lower, than the CTA, CTA-NF-1 and CTA-NF-2 which were 314 °C, 353 °C, 347 °C and 348 °C, respectively. The CTA and nanofibers show higher thermal stability and a wider range of degradation than the cellulose material, which was also shown in the work [24].

In electrospinning, along with such important parameters as the solution viscosity, the distance between the needle tip and the ground electrode, acceleration voltage, etc., the nature of solvent also plays an important role in the formation of nanofibers. The electrospinning of cellulose acetate in acetone was found to produce a short fibres or a “beads on the string” morphology. The rapidevaporation of solvent and the gelation of cellulose acetate solution, which clog the needle, are the causes of beading [25]. In order to solve this problem a new solvent system was used where ultrafine cellulose acetate fibers were successfully prepared via electrospinning of cellulose acetate in a mixed solvent of acetone/water at water contents of 10–15 wt % [26].

In our investigation, we used two binary mixed solvent systems: methylene chloride:ethanol and chloroform:acetone. The solvent system influences the solution properties and directly impacts the morphology and diameter of the resulting nanofibers. Being highly volatile the solvents used evaporated quickly during electrospinning, leading to the formation of thinner nanofibers. On the other hand, solvents with lower volatility may result in thicker fiber formation. Additionally, the choice of solvent system affects the drying kinetics and the solidification process of the electrospun fibers, which further influences their morphology, such as bead formation, uniformity, and alignment. Figure 4 displays SEM images of CTA-NF-1 and CTA-NF-2 nanofibers. The CTA-NF-1 nanofibers have a long uniform with a parallel grooved morphology, smooth surfaces, and few defects, and their size varies in the range of 200–700 nm. The grooved structure of nanofibers can be attributed to using solvents with different boiling temperatures in the mixed solvent system. Nano-

fibres with a similar surface texture were also formed from cellulose acetate butyrate solutions using a solvent mixture of acetone and N,N′-dimethylacetamide, and the authors explained this effect that there must be sufficient differences in the evaporation rate between the two solvents to initiate groove formation. It was discovered that the rapid evaporation of a highly volatile solvent from the polymer solution was crucial in the creation of surface voids, whereas the high viscosity of the residual solution after the solvent evaporation ensured the line surface to be formed following solidification [27].

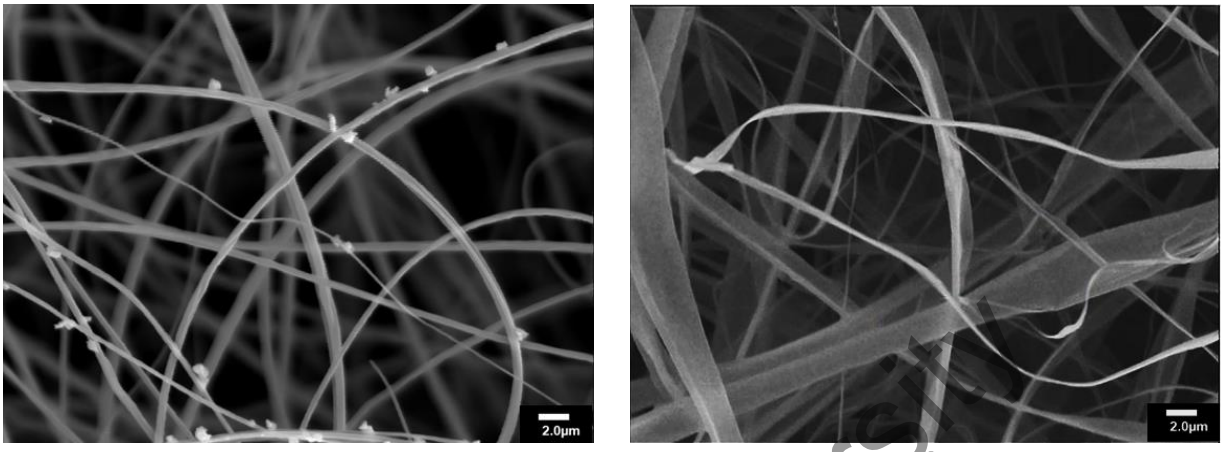

a *b*

Figure 4. SEM images of CTA-NF-1 (*a*) and CTA-NF-2 (*b*) nanofibers

The CTA-NF-2 nanofibers, ranging in size from 200 nm to 4 mkm, have a flat ribbon shape with two tubes (dumbbell shape) (Fig. 4, *b*), and it is related to the formation of the skin layer during electrospinning, which subsequently collapsed. Such ribbons have been formed by electrospinning various polymers [28]. The formation of this shape of nanofibers is associated with several parameters of the electrospinning process: the polymer molecular weight, the polymer solution concentration, the solution feed rate, the nature of the solvent, etc. [29–31]. Ribbon-like or flat nanofibres are produced while electrospinning with a more volatile solution [32-33]. The rapid vaporization of solvent results in the formation of a stable skin layer, as mentioned above, and the collapse of thin walls in the middle section of fibre, but this is insufficient to avoid material buildup at its sides [28].

Differences in capillary-porous structure parameters among LRC, CTA and CTA nanofibers can have significant implications for their respective applications in sorption studies. Sorption studies of the LCR, CTA, CTA-NF-1 and CTA-NF-2 using low molecular weight liquids (water) were carried out, and the capillary-porous structure parameters (monolayer capacity (X_m), specific surface area (S), total pore volume(W_o), average pore radius (r)) of the samples were calculated based on isotherms of water vapour sorption (Table 2).

Table 2

Sorption characteristics of samples

Sample	LRC	CTA	CTA-NF-1	CTA-NF-2
X_m, g/g	0.021	0.0036	0.0039	0.0081
S, m^2/g	86.0	12.83	13.89	28.94
W_o, cm^3/g	0.097	0.016	0.017	0.030
r, Å	45.5	16,76	18.56	24.12
Result presented as mean ±0.04 % standard deviation, n = 3				

The sorption process is a complex mechanism where several factors (capillary-porous, crystalline, supramolecular structure, content of non-cellulose substances) are simultaneously applied to the sorption kinetics. With its natural cellulose structure, LRC may exhibit high sorption capacity for water and other polar solvents due to its abundant hydroxyl (–OH) groups. The presence of hydroxyl groups in LRC provides opportunities for selective sorption of polar molecules or ions through hydrogen bonding and other interactions [8]. In case of CTA and nanofibers based on it, the parameters of the capillary-porous structure de-

crease in the series: CTA-NF-2 > CTA-NF-1 > CTA. The acetylation of cellulose in CTA reduces the number of hydroxyl groups available for sorption, resulting in lower sorption capacity compared to LRC. CTA nanofibers offer enhanced surface area and porosity compared to CTA, potentially leading to increased sorption capacity. Nanofibrous structures of CTA-NF-1 and CTA-NF-2 may exhibit faster sorption kinetics compared to CTA due to their high surface area and short diffusion pathways. The high surface-to-volume ratio of nanofibers can promote efficient sorption and adsorption of target molecules, making them suitable for applications such as filter material, adsorber, and sensing material.

Conclusions

The cellulose was extracted from licorice root waste and cellulose triacetate was successfully synthesized from licorice cellulose based on esterification method. In order to prepare cellulose nanofibers, the electrospinning has been studied using various solvent systems. In this study, a mixed solvent of methylene chloride/ethanol and chloroform/acetone were developed as a new solvent system for the electrospinning of CA nanofibers. The structural characteristics and morphology of LRC, CTA, CTA-NF-1 and CTA-NF-2 were investigated by the XRD, FT-IR, TGA, SEM, and compared. It was shown that the structure, properties, shape and size of nanofibers depend on using the solvent mixture. To the best of our knowledge, this is the first study reporting the formation nanofibers based on CTA, synthesized from licorice root cellulose. Such CTA nanofibers would be interesting for applications such as filtration materials due to their large surface area.

Funding

This research was funded by the Ministry of Higher Education, Science, and Innovation of the Republic of Uzbekistan (Grant No. FZ-4721055613).

*Author Information**

**The authors' names are presented in the following order: First Name, Middle Name and Last Name*

Siroj Shamsitdinovich Shakhabutdinov — Junior researcher, Institute of Polymer Chemistry and Physics, 100128, Tashkent, Uzbekistan; e-mail: sirojiddin_55@mail.ru; https://orcid.org/0000-0003-3804-9750

Svetlana MihaylovnaYugay — Candidate of chemical sciences, Senior researcher, Institute of Polymer Chemistry and Physics, 100128, Tashkent, Uzbekistan; e-mail: polymer@academy.uz; https://orcid.org/0000-0001-6829-4111

Nurbek Shodievich Ashurov — Candidate of physic-mathematic sciences, Senior researcher, Institute of Polymer Chemistry and Physics, 100128, Tashkent, Uzbekistan; e-mail: ansss72@mail.ru; https://orcid.org/0000-0001-5246-434X

Doniyor Jabborovich Ergashev — Junior researcher, Institute of Polymer Chemistry and Physics, 100128, Tashkent, Uzbekistan; e-mail: polymer@academy.uz; https://orcid.org/0000-0003-4547-9142

Abdumutolib Abdupatto o'g'li Atakhanov (*corresponding author*) — Doctor of technical sciences, Professor, Head of Laboratory "Physic and physic-chemical methods of investigation", Institute of Polymer Chemistry and Physics, 100128, Tashkent, Uzbekistan; e-mail: a-atakhanov@yandex.com; https://orcid.org/0000-0002-4975-3658

Sayyora Sharafovna Rashidova — Doctor of science, Professor, Academician, Director of Institute of Polymer Chemistry and Physics, 100128, Tashkent, Uzbekistan; e-mail: polymer@academy.uz; https://orcid.org/0000-0003-1667-4619

Author Contributions

The manuscript was written through contributions of all authors. All authors have given approval to the final version of the manuscript. CRediT: **Siroj Shamsitdinovich Shakhabutdinov** investigation, validation; **Svetlana Mihaylovna Yugay** investigation, methodology, visualization, writing-review; **Doniyor Jabborovich Ergashev** investigation, methodology, formal analysis; **Abdumutolib Abdupatto o'g'li Atakhanov** conceptualization, data curation, formal analysis, validation, writing-original draft, writing-review & editing; **Nurbek Shodievich Ashurov** conceptualization, data curation, investigation, methodology, visuali-

zation, writing-original draft, writing-review & editing; **Sayyora Sharafovna Rashidova** conceptualization, supervision, editing

Conflicts of Interest

The authors declare no conflict of interest.

References

1 Hernández-Becerra, E., Osorio, M., & Marín, D. (2023). Isolation of cellulose microfibers and nanofibers by mechanical fibrillation in a water-free solvent. *Cellulose*, 30: 4905–4923. https://doi.org/10.1007/s10570-023-05162-3

2 Wan, F., Wan, F., & Rizafizah O. (2019). Electrospun Cellulose Fibres and Applications. *Sains Malaysiana, 48*(7): 1459–1472. http://dx.doi.org/10.17576/jsm-2019-4807-15

3 Saidmuhamedova, M. Q., Turdiqulov, I. H., Atakhanov, A. A., Ashurov, N. Sh., Abdurazakov, M., Rashidova, S. Sh., & Surov, O. V. (2023). Biodegradable Polyethylene-Based Composites Filled with Cellulose Micro- and Nanoparticles. *Eurasian Journal of Chemistry, 110* (2): 94–106. https://doi.org/10.31489/2959-0663/2-23-16

4 Inukai, S., Kurokawa, N., & Hotta, A. (2018). Annealing and saponification of electrospun cellulose-acetate nanofibers used as reinforcement materials for composites. *Composites*, Part A, 113: 158–165. https://doi.org/10.1016/j.compositesa.2018.07.028

5 Kuzieva, M., Atakhanov, A. A., Shahobutdinav, S., Ashurov, N. S., Yunusov, K. E., & Guohua, (2023). Preparation of oxidized nanocellulose by using potassium dichromate. *Cellulose*, 30: 5657–5668. https://doi.org/10.1007/s10570-023-05222-8

6 Suhas, V. K., Gupta, P. J. M., Carrott, R. S., Chaudhary, M., & Kushwah, S. (2016). Cellulose: A review as natural, modified and activated carbon adsorbent. *Bioresource Technology*, 216: 1066–1076. https://doi.org/10.1016/j.biortech.2016.05.106

7 Lavanya, D., Kulkarni, P. K., Dixit, M., Raavi, P. K., & Krishna L. N. V. (2011). Sources of cellulose and their applications. *IJDFR*, 2(6).

8 Atakhanov, A. A., Mamadiyorov, B., Kuzieva, M., Yugay, S. M., Shahobutdinav, S., Ashurov, N. S., & Abdurazakov, M. (2019). Comparative studies of physic-chemical properties and structure of cotton cellulose and its modified forms. *Khimiia Rastitelnogo Syria*, 3: 5–13. https://doi.org/10.14258/jcprm.2019034554

9 Sun, J. X., Sun, X. F, Zhao, H., & Sun, R. C. (2004) Isolation and characterization of cellulose from sugarcane bagasse. *Polym. Degrad. and Stab., 84*(2): 331–339 https://doi.org/10.1016/j.polymdegradstab.2004.02.008

10 Daud, Z., Hatta, M. Z. M., Kassim, A., Awang, H., & Aripin A. M. (2013). Analysis the chemical composition and fiber morphology structure of corn stalk. *Austr. J. Basic and Appl. Sci.*, 7: 401–405.

11 Deutch., M. R., Grimm, D., Wehland., M., Infanger, M., & Krüger, M. (2019). Bioactive Candy: Effects of Licorice on the Cardiovascular System. *Foods, 14*(8, 10): 495. https://doi.org/10.3390/foods8100495

12 Alimova, D., Nabieva, I., & Atakhanov A. (2023). Paper production from the waste of medicinal plants. *E3S Web of Conferences*, 452: 05013. https://doi.org/10.1051/e3sconf/202345205013

13 Saeed, U., Dawood, U., & Ali, A. M. (2021). Cellulose triacetate fiber-reinforced polystyrene composite. *J. Thermoplast. Compos. Mater*, 34: 707–721. https://doi.org/10.1177/0892705719847249.

14 Goetz, L. A., Jalvo, B., Rosal, R., & Mathew, A. P. (2016). Superhydrophilic anti-fouling electrospun cellulose acetate membranes coated with chitin nanocrystals for water filtration. *Journal of Membrane Science*, 510, 238–248. https://doi.org/10.1016/j.memsci.2016.02.069

15 Greiner, A., & Wendorff, J. H., (2007). Electrospinning: a fascinating method for the preparation of ultrathin fibers. *Angewandte Chemie Inter. Edit*. 46: 5670–5703. https://doi.org/10.1002/anie.200604646.

16 Xue, J., Wu, T., Dai, Y., & Xia, Y. (2019). Electrospinning and Electrospun Nanofibers: Methods, Materials, and Applications. *Chem Rev, 119*(8): 5298–5415. https://doi.org/10.1021/acs.chemrev.8b00593

17 Jiang, L., Li, K., Yang, H., Liu, X., Li, W., Xu, W., & Deng, B. (2020). Improving mechanical properties of electrospun cellulose acetate nanofiber membranes by cellulose nanocrystals with and without polyvinylpyrrolidone. *Cellulose*, 27: 955–967. https://doi.org/10.1007/s10570-019-02830-1

18 Shaikh, H. M., Anis, A., & Poulose, A. M. (2022). Synthesis and Characterization of Cellulose Triacetate Obtained from Date Palm (Phoenix dactylifera L.) Trunk Mesh-Derived Cellulose. *Molecules, 27*(4): 1434. https://doi.org/10.3390/molecules27041434

19 Frey, M. W. (2008). Electrospinning cellulose and cellulose derivatives. *Polym Rev., 48*(2): 378–391. https://doi.org/10.1080/15583720802022281

20 Abdulhanan, B., Muhammed, T. I., Benjamin, O. A., & Bello, M. (2016). Acetylation of Cotton Stalk for Cellulose Acetate Production. *ASRJETS, 15*(1): 137–150.

21 Ifuku, S., Nogi, M., Abe, K., Handa, K., Nakatsubo, F., & Yano, H. (2007). Surface Modification of Bacterial Cellulose Nanofibers for Property Enhancement of Optically Transparent Composites: Dependence on Acetyl-Group DS. *Biomacromolecules, 8*(6), 1973–1978. https://doi.org/10.1021/bm070113b

22 Kargarzadeh, H., Ahmad, I., Abdullah, I., Dufresne, A., Zainudin, S. Y., & Sheltami R. M. (2012). Effects of hydrolysis conditions on the morphology, crystallinity, and thermal stability of cellulose nanocrystals extracted from kenaf bast fibers. *Cellulose*, 19: 855–866. https://doi.org/10.1007/s10570-012-9684-6

23 Barud, H. S., de Araújo Júnior, A. M., Santos, D. B., de Assunção, R. M. N., Meireles, C. S., Cerqueira, D. A., Rodrigues Filho, G., Ribeiro, C. A., Messaddeq, Y., & Ribeiro, S. J. L. Thermal behavior of cellulose acetate produced from homogeneous acetylation of bacterial cellulose. (2008). *Thermochim. Acta*., 471: 61–69. https://doi.org/10.1016/j.tca.2008.02.009.

24 Chen, J., Xu, J., Wang, K., Cao, X., & Sun, R. (2016). Cellulose acetate fibers prepared from different raw materials with rapid synthesis method. *Carbohydr. Polym*., 137: 685–692. https://doi.org/10.1016/j.carbpol.2015.11.034.

25 Liu, H., Hsieh, Y. L. (2002). Ultrafine fibrous cellulose membranes from electrospinning of cellulose acetate. J. Polym. Sci. Part B: Polym. Phys., 40: 2119–2129. https://doi.org/10.1002/polb.10261

26 Son, W. K., Youk, J. H., Lee, T. S., & Park, W. H. (2004). Electrospinning of ultrafine cellulose acetate fibers: Studies of a new solvent system and deacetylation of ultrafine cellulose acetate fibers. J. Polym. Sci. Part B: Polym. Phys., 42: 5–11. https://doi.org/10.1002/polb.10668

27 Huang, C., Tang, Y., Liu, X., Sutti, A., Ke, Q., Mo, X., Wang, X., Morsic, Y., & Lin, T. (2011). Electrospinning of nanofibres with parallel line surface texture for improvement of nerve cell growth. *Soft Matter*., 7: 10812–10817. https://doi.org/10.1039/C1SM06430D

28 Koombhongse, S., Liu, W., & Reneker, D. H. (2001). Flat polymer ribbons and other shapes by electrospinning. J. Polym. Sci. Part B, 39: 2598–2606. https://doi.org/10.1002/POLB.10015

29 Dhanalakshmi, M., & Jog, J. P. (2008). Preparation and characterization of electrospun fibers of Nylon 11. eXPRESS Polym. Lett., 2(8): 540–545. https://doi.org/10.3144/expresspolymlett.2008.65

30 Koski, A., Yim, K., & Shivkumar, S. (2004). Effect of molecular weight on fibrous PVA produced by electrospinning. *Mater. Lett.*, *58*(3-4): 493–497. https://doi.org/10.1016/S0167-577X(03)00532-9

31 Chen, S. H., Chang, Y., Lee, K. R., & Lai, J. Y. (2014). A three-dimensional dual-layer nano/microfibrous structure of electrospun chitosan/poly(D,L-lactide) membrane for the improvement of cytocompatibility. *J. Membr.Sci*., 450: 224–234. https://doi.org/10.1016/j.memsci.2013.08.007

32 Ghorani, B., Russell, S. J., & Goswami, P. (2013). Controlled morphology and mechanical characterisation of electrospun cellulose acetate fibre webs. *Int. J. Polym. Sci.* ID 256161. https://doi.org/10.1155/2013/256161

33 Choktaweesap, N., Arayanarakul, K., Aht-Ong, D., Meechaisue, C., & Supaphol, P. (2007). Electrospun gelatin fibers: effect of solvent system on morphology and fiber diameters. *Polym. J. 39*: 622–631. https://doi.org/10.1295/polymj.PJ2006190